J Mater Sci (2007) 42:914–922
DOI 10.1007/s10853-006-0009-8

Effect of Ni loading and reaction temperature on the formation of carbon nanotubes from methane catalytic decomposition over Ni/SiO_2

Lúcia K. Noda · Norberto S. Gonçalves · Antoninho Valentini · Luiz F. D. Probst · Rusiene M. de Almeida

Received: 27 October 2005 / Accepted: 14 March 2006 / Published online: 31 December 2006

Abstract Since their discovery carbon nanotubes (CNT) have attracted much attention due to their singular physical, mechanical and chemical properties. Catalytic chemical vapor deposition (CCVD) of hydrocarbons over metal catalysts is the most promising method for the synthesis of CNT, because of the advantages of low cost and large-scale production and the relatively low temperature used in the process, compared to the other methods (laser ablation and discharge between graphite electrodes). In this study, CNT were synthesized by CCVD using Ni supported on SiO_2 as a catalyst. The carbon deposited in the reaction was analyzed by Raman spectroscopy, thermogravimetric analysis (TGA), scanning electron microscopy (SEM) and transmission electron microscopy (TEM). The effects of reaction temperature and Ni loading on the carbon nanotube formation were evaluated. The catalyst with 5% Ni favored high yield of CNT at lower temperature, with abundant ''multi-walled carbon nanotubes'' (MWNTs) at 625 °C, while single-walled carbon nanotubes (SWNTs) and MWNTs were obtained at 650 °C. With an increase in the reaction temperature a marked decrease in the yield of CNT was observed, probably due to the sintering of the catalyst. The catalyst with 1% Ni gave SWNTs with a high degree of order at all reaction temperatures, but in low quantity.

L. K. Noda (✉) · N. S. Gonçalves · L. F. D. Probst · R. M. de Almeida
Laboratory of Heterogeneous Catalysis, Chemistry Department, Universidade Federal de Santa Catarina, Florianopolis 88040-900 SC, Brazil
e-mail: lucia@qmc.ufsc.br

A. Valentini
Department of Analytical and Physical Chemistry, Universidade Federal do Ceará, Campus do Pici, Fortaleza 60455-760 CE, Brazil

Introduction

Since Iijima's discovery of carbon nanotubes (CNT) in 1991 [1], there has been a growing interest in these materials. Their remarkable electrical and mechanical properties have led to opportunities for several applications, such as in nanoelectronic devices, field emission devices, high strength composites, etc. CNT are formed by rolled up graphene sheets forming tubes with diameters of a few nanometers. They are classified as single walled (SWNT) and multi-walled (MWNT) carbon nanotubes, the former being the one of most interest. Several methods of CNT synthesis have been investigated, such as discharge between two graphite electrodes [2], laser ablation [3], hydrocarbon decomposition [4], and catalytic chemical vapor decomposition, CCVD [5, 6]. The first two methods give high quality SWNTs, but they are more expensive and yield much lower quantities of CNTs than CCVD. Thus, CCVD seems to be the best choice for large-scale production of CNTs at low cost.

In Table 1, examples of CNT syntheses by CCVD method are given. Paigney et al. [7] reported SWNT and MWNT synthesis from methane catalytic decomposition using Fe nanoparticles supported on SiO_2 as a catalyst. Isolated SWNTs were obtained by methane CCVD on Fe_2O_3 [8]. Hafner et al. [9] synthesized SWNTs in mg/h in CO and ethylene CCVD on Mo and Fe:Mo at 700 °C and 850 °C. Dai et al. [10] obtained

Table 1 Examples of CNT syntheses by CCVD method

Reagent	Catalyst	Kind of nanotube	T (°C)	Ref.
Methane	Fe/SiO_2	SWNTs and MWNTs	800	[7]
Methane	Fe_2O_3	Isolated SWNT	1000	[8]
CO and ethylene	Mo and Fe:Mo	SWNT	700 and 800	[9]
Methane	Fe/Al_2O_3	SWNT	900	[10]
Methane	Co/MgO, Ni/MgO, Fe/MgO and Co–Fe/MgO	SWNT in large scale	1000	[11]
Methane, hexane, cyclohexane,benzene, naphtalene, antharacene	Fe/MgO	SWNT	500–850	[12]
Acetylene	Co–Mo/MgO	SWNT	800	[13]
Ethanol	Fe/SiO_2 and Co/SiO_2	SWNT	750	[14]

high qualities SWNTs in methane CCVD on an alumina supported Fe catalyst at 900 °C. Colomer et al. [11] obtained SWNTs in large scale from methane CCVD using Co, Ni and Fe supported on MgO and Co–Fe as catalysts at 1,000 °C. Besides methane, ethylene and CO, other compounds can be used as carbon sources in CCVD. Li et al. [12] investigated SWNT formation from methane, hexane, cyclohexane, benzene, naphtalene and anthracene decomposition on Fe supported on MgO at 500–850 °C. Shajahan et al. [13] reported SWNT formation from acetylene decomposition on Co–Mo/MgO at 800 °C, while Murakami et al. [14] used ethanol decomposition to obtain SWNTs.

Nowadays, one of the most important research activities is the direct synthesis of CNTs on appropriate substrates aiming at their integration into electronic devices [15]. To achieve a high degree of compatibility with standard semiconductor processes it is crucial that the CNT growth temperature is as low as possible, maintaining a high yield and good quality. CCVD is the most suitable method for CNT synthesis at low temperatures, because using other techniques the temperatures attained are much higher. Among the metals used as catalysts in CNT synthesis, Ni is the one that needs the lowest temperature [16, 17], probably due to its lower melting point, compared to Fe and Co.

In this paper the CNT formation from catalytic decomposition of methane at several temperatures, using Ni supported on SiO_2, with 1% and 5% of Ni, is reported. Characterization of the samples after reaction was performed by Raman spectroscopy, thermogravimetric analysis (TGA), scanning and transmission electron microscopy (TEM).

Experimental

The SiO_2 supported Ni catalysts were prepared by the wet impregnation method. Nickel nitrate (Fluka Chemika), Aerosil 200 (Degussa) and water were mixed in appropriate amounts and put in the round-bottomed flask of a rotoevaporator system. The water was pumped off until the mixture became a paste, which was then placed in an oven at 90 °C for 18 h. The dried samples were then calcinated at 500 °C in a tubular furnace for 1 h in a flow of Ne and He. Two samples with 1% and 5% of Ni, calculated as percentage of Ni by weight in relation to the total weight of the sample, were prepared, being named as $NiSiO_2$-1 and $NiSiO_2$-5, respectively.

The methane catalytic decomposition was carried out in a tubular fixed bed quartz reactor at 625 °C, 650 °C, 700 °C, 750 °C and 800 °C. Fifty milligrams of catalyst ($NiSiO_2$-1 or $NiSiO_2$-5) was previously activated for 1 h, at the same temperature as that of the reaction, with a heating rate from ambient temperature until the final temperature of 10 °C min^{-1}, in a flow of H_2. H_2 was then replaced with a mixture of N_2 and CH_4 with a total flow of 35 cc min^{-1}, which was kept in contact with the catalyst while catalytic activity was observed (around 15 min). The methane conversion was analyzed with a Shimadzu GC, equipped with a packed column (Porapak Q and PM 5A) and a thermal conductivity detector. After the reaction the catalysts along with the solid products were analyzed by Raman spectroscopy, thermogravimetric analysis, scanning and transmission electron microscopy.

The thermogravimetric analyses were performed in a Shimadzu TGA-50 equipment, in an oxidant atmosphere (synthetic air), with a temperature range of 25–900 °C, and a heating rate of 10 °C/min.

The Raman spectra were obtained with a Renishaw Raman System 3000 instrument coupled to a microscope (Olympus BH-2) and with a CCD detector. The spectra were excited by the 632.8 nm line of a He–Ne laser (Spectra-Physics) with an estimated power incident on the sample of 1 mW. The size of the laser spot on the sample was around 2 μm.

The SEM analyses were performed with a JEOL JSM-6360 instrument, operating at 20 kV. The samples

were fixed in a copper tape, with a layer of gold deposited on it, in a vacuum chamber.

TEM analyses were carried out with a JEOL 1200 EX-II instrument, operating at 60 kV. The powdered samples were suspended in acetonitrile, sonicated for some minutes and then deposited over a parlodium covered copper grid. The samples were dried at room temperature for 24 h.

Results and discussion

Thermogravimetric analyses

SWNTs, MWNTs and other carbon materials have characteristic weight loss temperatures, when submitted to TGA in an oxidant atmosphere [18, 19]. The carbon materials formed after catalytic reactions during methane decomposition were quantitatively determined.

The thermogravimetric analyses of sample $NiSiO_2$-5 after the catalytic reactions, Fig. 1, show first derivative peaks of weight loss (DrTGA) in the temperature range of 450–700 °C. In the TGA curve of the sample after reaction at 625 °C, a considerable weight loss, around 45%, was observed, with a peak in the DrTGA curve at 652 °C, characteristic of MWNT oxidation [18]. The sample after the reaction at 650 °C showed a 7.5% weight loss, which has two components, as can be seen in the DrTGA curve, one peaking at 665 °C and the other being a shoulder at around 510 °C. The

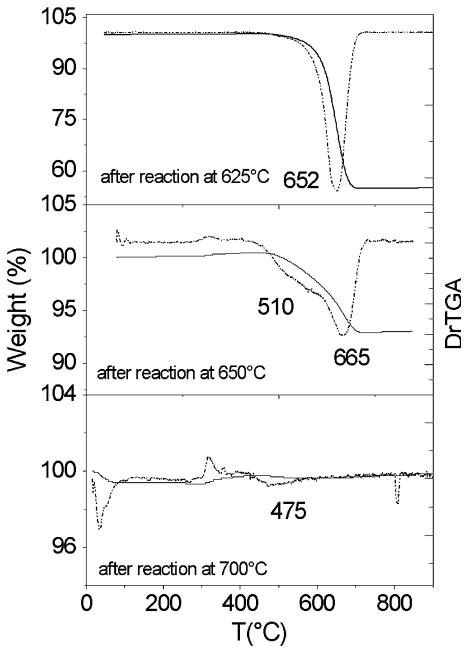

Fig. 1 Thermogravimetric curves, TGA (continuous line) and first derivative curves, DrTGA (broken line) of $NiSiO_2$-5 sample after catalytic decomposition of methane

former could be assigned to MWNTs and the latter to SWNTs [19]. The sample after reaction at 700 °C has a very low weight loss, around 1%, which peaks at around 475 °C, which may be due to the presence SWNTs.

The TGA curves of all the samples obtained after catalytic reactions using $NiSiO_2$-1 as the catalyst showed low weight loss, around 1%, and for this reason they are not shown.

Raman spectroscopy

The characteristic features of the Raman spectra of the fundamental modes of CNTs are summarized as follows. A strong band at around 1590 cm^{-1}, the tangential C–C stretching mode (G-band), is observed for both MWNTs and SWNTs. In the Raman spectra of metallic SWNTs, the G band appears as a doublet, with a characteristic band at around 1550 cm^{-1}, besides the band at 1590 cm^{-1} [20]. The D band in the interval 1280–1350 cm^{-1} is observed in MWNTs and defective SWNTs, but is also present in other low ordered carbon materials. The low frequency bands (100–300 cm^{-1}) are due to the radial breathing mode, these being unique to SWNTs; from their frequencies it is possible to calculate the SWNT diameter [21].

The Raman spectra in the low frequency region (50–300 cm^{-1}) and in the high frequency region (1200–1850 cm^{-1}) of samples $NiSiO_2$-5 and $NiSiO_2$-1 after reactions at 625 °C, 650 °C, 700 °C, 750 °C and 800 °C, are shown in Figs. 2 and 3, respectively.

$NiSiO_2$-5

After reaction at 625 °C, in the low frequency region, practically no bands are observed (only a very weak one at 186 cm^{-1}), indicating that SWNTs are absent. In the high frequency region, broad bands at 1580 cm^{-1} and 1329 cm^{-1}, assigned to the G and D modes, respectively, are seen, with the D band being more intense than the G band. The band at 1550 cm^{-1}, typical of metallic SWNTs, is not observed. These bands confirm that SWNTs are really absent and that the spectrum may be due to MWNTs or amorphous carbon. However, TGA analysis indicated the presence of MWNTs, ruling out the presence of amorphous carbon. Thus, the observed Raman spectrum features must be due to the presence of MWNTs.

The sample after reaction at 650 °C presents very significant differences. In the low frequency region, the radial breathing modes at 189.2, 259.3, 279.1 and 292.0 cm^{-1}, characteristic of SWNTs, are observed. Using the frequencies of these modes in cm^{-1}, the

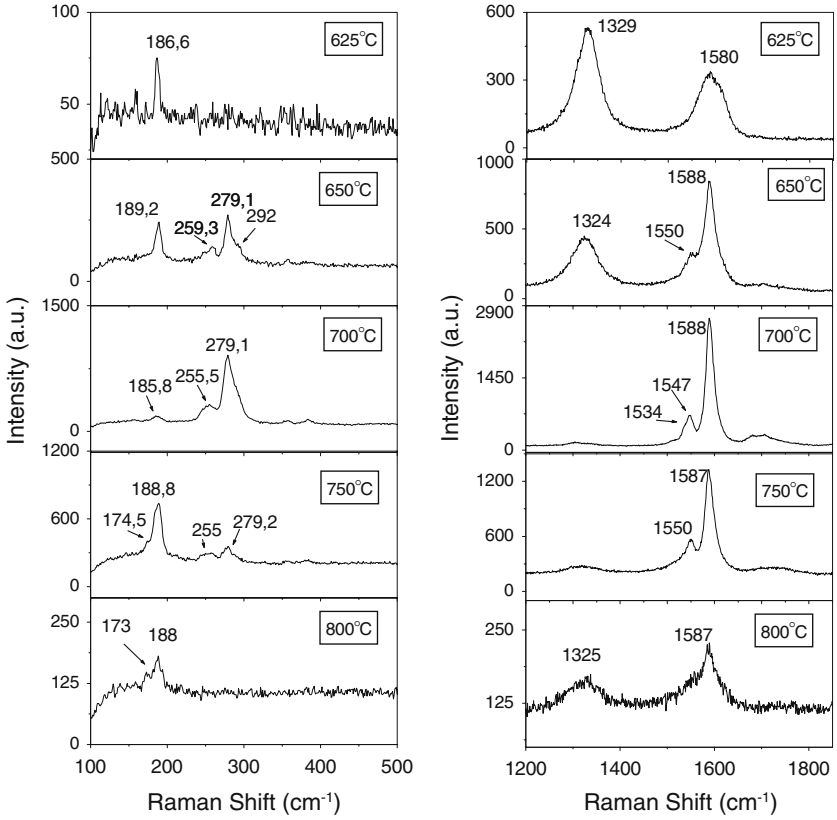

Fig. 2 Raman spectra of $NiSiO_2$-5 after methane catalytic decomposition, at the indicated reaction temperatures. The low frequency region and the high frequency region are shown on the left and on the right, respectively

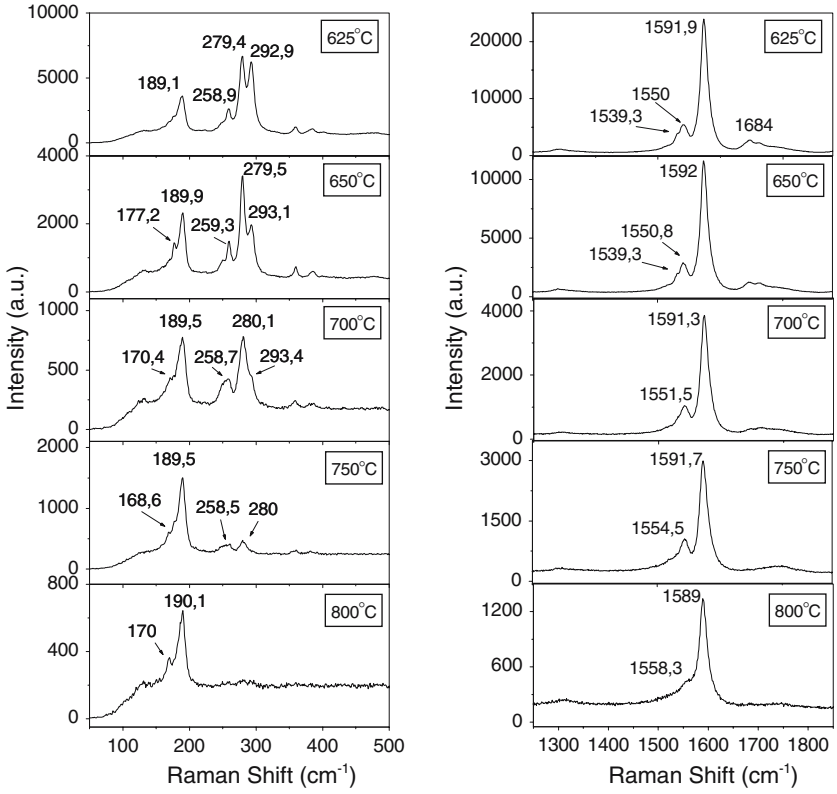

Fig. 3 Raman spectra of $NiSiO_2$-1 after methane catalytic decomposition, at the indicated reaction temperatures. The low frequency region and the high frequency region are shown on the left and on the right, respectively

Table 2 SWNT diameter obtained from the frequency of the Raman radial breathing mode, using the equation proposed by Alvarez [21]

Sample	T (°C)	ω (cm^{-1})	Diameter (nm)
$NiSiO_2$-1	625–650	189.4	1.22
		259	0.89
		279.2	0.82
		292.8	0.78
	700	189.4	1.22
		279.2	0.82
$NiSiO_2$-5	625	–	–
	650	189	1.22
		255	0.90
		279	0.82
	700	185.9	1.25
		255	0.90
		279	0.82

SWNT diameter in nanometers, d (nm), can be calculated from the equation: ω (cm^{-1}) = 6.5 + 223.75/d(nm) [21]. In Table 2, the calculated diameters are shown for samples after reaction at the different temperatures. In the high frequency region, the G and D bands are narrower and the D band (1324 cm^{-1}) is weaker than the G band. (1588 cm^{-1}), but still has a considerable intensity. A band at 1550 cm^{-1}, characteristic of SWNTs, then appears. It can be concluded from these data that this sample contains SWNTs and probably MWNTs, because of the intensity of the D band. Thus, the Raman spectrum confirms the TGA analysis, which presented two weight loss peaks, due to two different carbon forms.

The Raman spectrum of the sample after reaction at a 700 °C has a considerably higher intensity than the spectrum of the sample after reaction at 650 °C, except for the intensity of the D band that decreased greatly. These data show that the CNT are SWNTs with a high degree of ordering. The tubes with smaller diameters (radial breathing mode frequencies at 270–290 cm^{-1}) are predominant in relation to the larger diameter tubes (radial breathing frequencies at 170–190 cm^{-1}), as can be seen from the intensities of the bands in the low frequency region. Although the TGA analysis showed that the amount of carbon is low, the Raman signal is very high, because of the high Raman cross-section of the SWNTs present in this sample, which is highly ordered.

The Raman spectrum of the sample after the reaction at 750 °C shows two main differences in relation to the spectrum of the sample after reaction at 700 °C. The whole spectrum is weaker and the band at around 189 cm^{-1} in the low frequency region is now predominant, indicating that the carbon nanotube diameters have shifted to higher values.

Table 3 I_G/I_D (relative intensity of G and D bands)

T (°C)	$NiSiO_2$-5	$NiSiO_2$-1
625	0.58	48
650	2.1	43
700	37	55
750	15	32
800	2.3	21

The whole Raman spectrum of the sample after reaction at 800 °C shows an abrupt decrease. The results from the TGA analysis and Raman spectroscopy, showing a decrease in the amount of carbon with an increase in the reaction temperature, may be explained by catalyst deactivation due to a sintering process. This hypothesis will be discussed later in detail in the SEM and TEM results.

An interesting feature of the Raman spectra in the low frequency region for the samples formed at all the investigated temperatures is the presence of two distinct frequency ranges, one at around 170–190 cm^{-1} and the other at around 250–290 cm^{-1}, with a ''gap'' between them. The bands in the lower frequency range are assigned to the semiconducting SWNTs of larger diameters, whose E_{22} transition is in resonance with the excitation at 1.96 eV. The bands in the higher frequency range are assigned to the metallic SWNTs of smaller diameters, whose E_{11} transition is in resonance with the exciting radiation [22].

The relative intensities of the G and D bands, I_G/I_D, which is a measure of the degree of perfection of SWNTs and also of the presence of other carbon forms, were measured for all the samples and are shown in Table 3. The highest I_G/I_D value for sample $NiSiO_2$-5 was found after reaction at 700 °C, indicating that SWNTs formed at this reaction temperature are the most ordered, while the lowest value was found after reaction at 625 °C.

$NiSiO_2$-1

The Raman spectra of sample $NiSiO_2$-1 (Fig. 3) for all the reaction temperatures show the presence of SWNTs, contrasting to sample $NiSiO_2$-5, where MWNTs or mixtures of SWNTs and MWNTs were present at lower temperatures. The highest signal was obtained at 625 °C where the D band was weak, indicating that the nanotubes are well ordered. On increasing the reaction temperature the Raman signal decreases gradually, with a behavior similar to that observed for sample $NiSiO_2$-5, which may be explained by the occurrence of the same process, catalyst deactivation, caused probably by catalyst sintering.

On analyzing the bands in the low frequency region it can be seen that the tubes with smaller diameters predominate at the lower temperatures while tubes with larger diameters predominate at the higher temperatures. This behavior was observed for sample $NiSiO_2$-5 and has been observed for other catalysts, for instance, Maruyama et al. [23] who studied SWNT formation from ethanol decomposition over zeolite Y with Fe and Co.

Electron microscopy

SEM of $NiSiO_2$-5

The images obtained from SEM analysis of sample $NiSiO_2$-5 after reaction at 625 °C, 650 °C, 700 °C and 750 °C are shown in Fig. 4.

In the sample after reaction at 625 °C (Fig. 4a) abundant entangled carbon filaments are observed, with estimated average diameters of 100 nm (with the formation of a few loops). This is in agreement with the high weight loss observed in the TGA analysis. The SEM images also confirm the Raman spectra results, from which MWNT formation was postulated. The whole catalyst surface is covered by these filaments, which prevent the observation of its morphology.

After reaction at 650°C (Fig. 4b), a significant decrease in the amount of filaments on the surface is observed. The diameters of these tubes, between 50 nm and 100 nm, are a little smaller than those of the sample formed at 625 °C. The decrease in the amount of tubes is in agreement with the TGA analysis, which also showed lower weight loss than that of the sample at 625 °C. Since the Raman spectra showed a mixture of MWNTs and SWNTs, the tubes observed by SEM could be assigned to MWNTs. The catalyst surface can be visualized, although it is not well defined. There are some grains with light color, with an estimated size between 1 μm and 2 μm.

After reaction at 700 °C (Fig. 4c), there were fewer, more aligned, carbon filaments. The lower amount of carbon filaments is in agreement with the TGA analysis, which showed a weight loss of only around 1%. The catalyst surface was clearly visible, consisting of an agglomeration of grains, with an average diameter of 100 nm and also some larger grains (with lighter color), probably indicating the beginning of the sintering process.

After reaction at 750 °C (Fig. 4d), the carbon filaments had almost disappeared. Nevertheless, the Raman spectrum detected the presence of SWNTs, because the sample area covered by the laser spot is larger when compared to the area sampled by SEM and also because of the very high Raman scattering cross-section of SWNTs. The sintering process continues, as can be seen by the increase in the average size of the sample grains, in the range of 100–200 nm.

TEM of sample $NiSiO_2$-5

On the TEM image of sample $NiSiO_2$-5 after reaction at 625 °C (Fig. 5a), hollow tubes with an average diameter of 20 nm can be observed. The hollow region is narrower than the walls, suggesting that the tubes are MWNTs. Some spherical dark particles encapsulated inside the tubes are seen, probably Ni particles. The

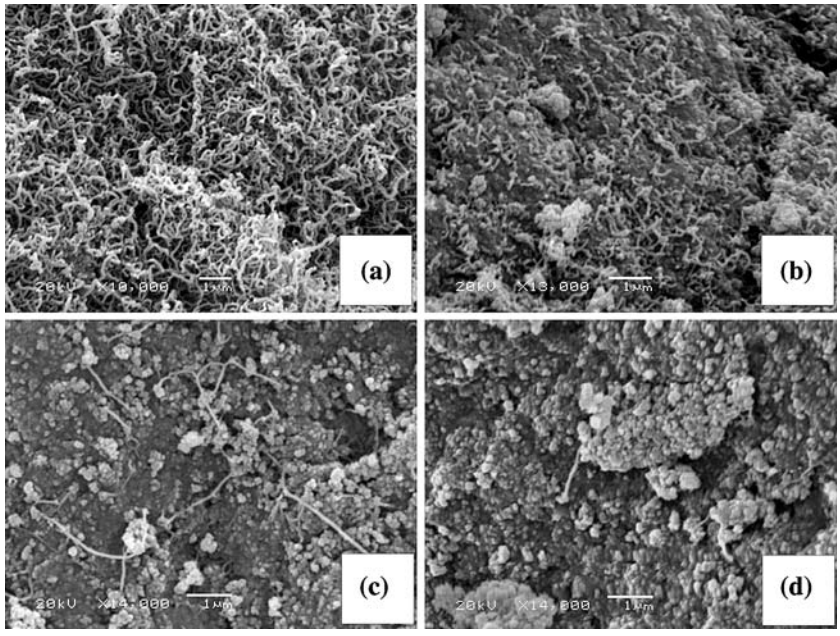

Fig. 4 SEM of sample $NiSiO_2$-5 after the indicated reaction temperatures: (a) 625 °C, (b) 650 °C, (c) 700 °C and (d) 750 °C

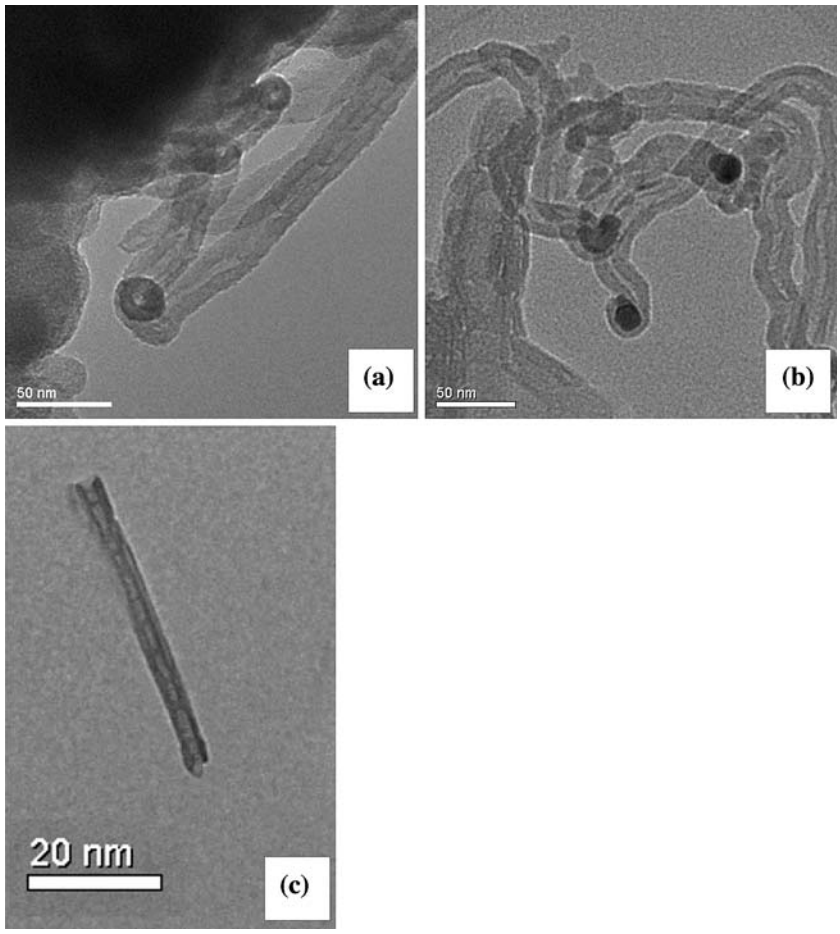

Fig. 5 TEM of sample $NiSiO_2$-5 after the indicated reaction temperatures: (a) 625 °C, (b) and (c) 650 °C

images of the sample after reaction at 650 °C are shown in Figs. 5b and c. Hollow tubes with an average diameter of 25 nm and also with encapsulated Ni particles are observed in Fig. 5b, similar to those seen in Fig. 5a. In Fig. 5c, a thin hollow tube with around 4 nm of diameter is observed, probably a MWNT with few walls. Although SWNTs are not observed by electron microscopy, they were detected by Raman spectroscopy, because of the largest area sampled by the laser beam, along with the high Raman cross-section of the SWNTs.

After reaction at 700 °C very sparse nanotubes can be seen in the image, Fig. 6a, which is in agreement with the TGA analysis; at some points cubic nickel monocrystals (with around 0.2 μm edge), not observed at lower reaction temperatures, are now seen. After reaction at 750 °C no nanotubes are observed, Fig. 6b, however, amorphous carbon is now present, as in the upper region of the image [24]. This amorphous carbon was not detected by Raman spectroscopy due to its very low quantity in addition to its low Raman scattering cross-section. Larger nickel crystals with 1 μm edges are seen at this higher temperature, Fig. 6c, indicating that the sintering process, started at a lower temperature, is now more advanced.

SEM of sample $NiSiO_2$-1

The main feature of the images for samples after the three reaction temperatures, Fig. 7, is the low amount of carbon filaments, in agreement with the TGA analyses. The filaments are not entangled and are well ordered, which is consistent with the Raman spectrum (Fig. 3), which showed SWNTs with a high degree of ordering.

Conclusions

The catalytic decomposition of methane aiming at the formation of CNT showed different behaviors depending on the Ni loading of the catalyst and on the reaction temperature. The reaction using a catalyst with 5% Ni, $NiSiO_2$-5, favored the formation of MWNTs at a lower reaction temperature. The SWNTs are formed with increasing temperature, but when

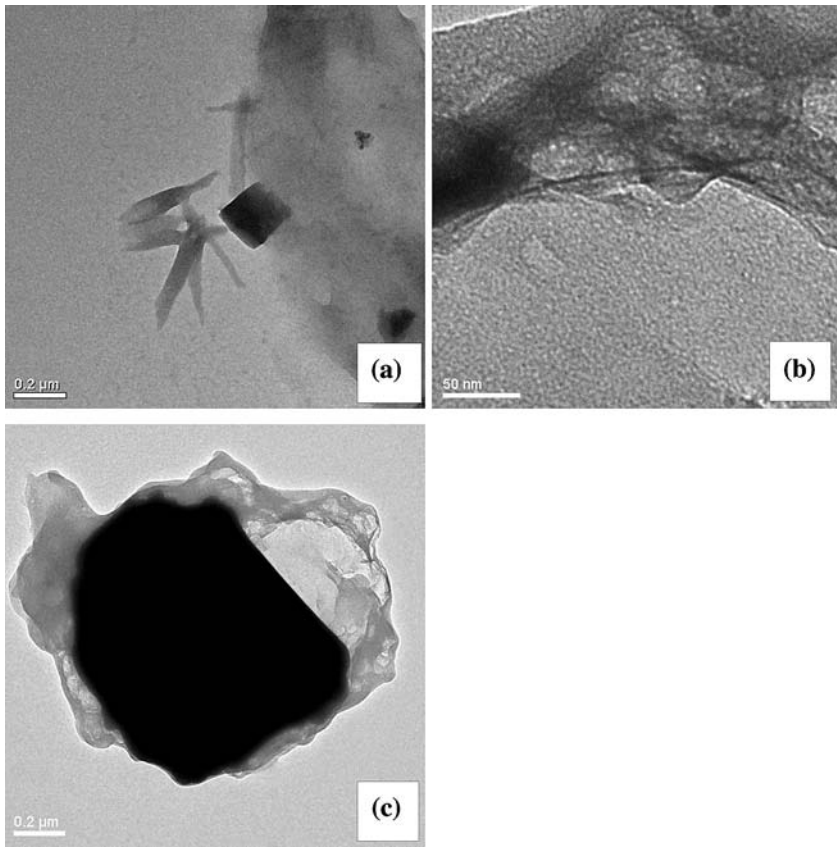

Fig. 6 TEM of sample $NiSiO_2$-5 after the reaction temperatures: (a) 700 °C, (b) and (c) 750 °C

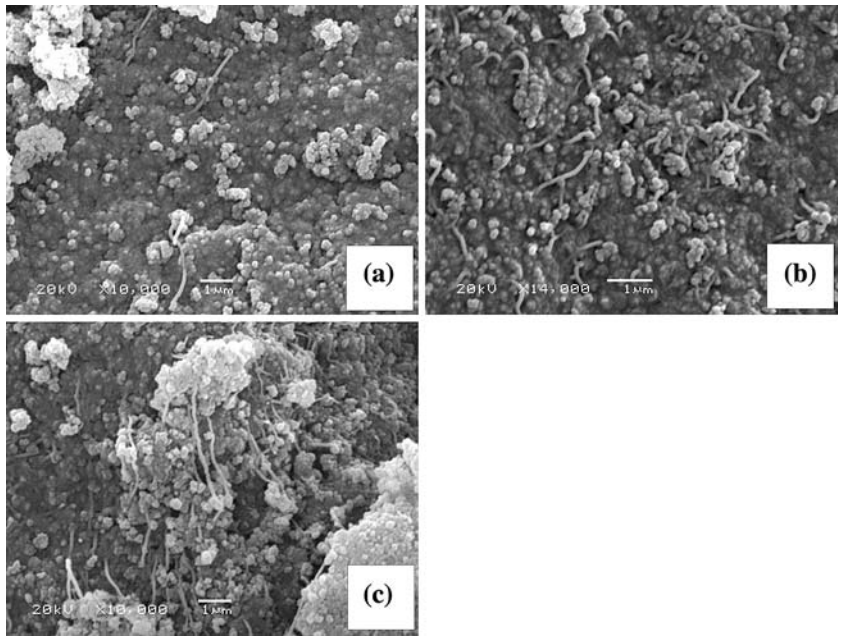

Fig. 7 SEM of sample $NiSiO_2$-1 after the reaction temperatures: (a) 625 °C, (b) 650 °C and (c) 700 °C

they predominate the amount formed in the reaction is very low. The catalyst with 1% Ni, $NiSiO_2$-1, favored the formation of SWNTs at all the reaction temperatures, but in very low quantities. With higher temperatures the amount of nanotubes decreased significantly for reactions with the two catalysts, probably due to catalyst deactivation, caused by a sintering process.

Acknowledgements Thanks to CNPq, Prodoc CAPES, Laboratory of Molecular Spectroscopy of Chemistry Institute, São Paulo University for the utilization of Renishaw Raman System 3000.

References

1. Iijima S (1991) Nature 354:56
2. Iijima S, Ichihashi T (1993) Nature 363:603
3. Guo T, Nikolaev P, Thess A, Colbert DT, Smalley RE (1995) Chem Phys Lett 243:49
4. Kong J, Cassel AM, Dai H (1998) Chem Phys Lett 292:4
5. Dai HX, Rinzler P, Nikolacv P, Thess A, Colbert DT, Smalley RE (1996) Chem Phys Lett 260:471
6. Colomer JF, Bister G, Willems I, Konya Z, Fonseca A, Van Tendeloo G, Nagy JB (1999) Chem Commun 1343
7. Peigney A, Laurent Ch, Dobigcon F, Roussel A (1997) J Mater Res 12:613
8. Kong J, Cassel AM, Dai H (1998) Chem Phys Lett 292:567
9. Hafner JH, Bronikowski MJ, Azamian BR, Nikolaev P, Rinzler AG, Colbert DT, Smith KA, Smalley RE (1998) Chem Phys Lett 296:195
10. Cassel AM, Kong JA, Dai HJ (1999) Phys Chem B103:6484
11. Colomer JF, Stephan C, Lefrant S, Van Tendeloo G, Willems I, Kónya Z, Fonseca A, Laurent C, Nagy JB (2000) Chem Phys Lett 317:83
12. Li Q, Yan H, Zhang J, Liu Z (2004) Carbon 42:829
13. Shajahan M, Mo YH, Kibria AKMF, Kim MJ, Nahm KS (2004) Carbon 42:2245
14. Murakami Y, Yamakita S, Okubo T, Maruyama S (2003) Chem Phys Lett 375:393
15. Javey A, Kim H, Brink M, Wang Q, Ural A, Guo J, Mcintyre P, Mceuen P, Lundstrom M, Dai H (2002) Nat Mater 1:241
16. Seidel R, Liebau M, Duesberg BS, Kreupl F, Unger E, Graham AP, Hoenlein W, Pompe W (2003) Nanoletters 3:965
17. Seidel R, Duesberg GS, Unger E, Graham AP, Liebau M, Kreupl F (2004) J Phys Chem B108:1888
18. Tang S, Zhong Z, Xiong Z, Liu L, Lin J, Shen ZX, Tan KL (2001) Chem Phys Lett 350:19
19. Kitiyanan B, Alvarez WE, Harwel JH, Resasco DE (2000) Chem Phys Lett 317:497
20. Pimenta MA, Marucci A, Empedocles S, Bawendi M, Hanlon EB, Rao AM, Eklund PC, Smalley G, Dresselhaus RE, Dresselhaus MS (1998) Phys Rev B58:R16012
21. Alvarez L, Righi A, Guillard T, Rols S, Anglaret E, Laplaze D, Dauvajol JL (2000) Chem Phys Lett 316:186
22. Liao H, Hafner JH (2004) J Phys Chem B108:6941
23. Maruyama S, Kojima R, Miyauchi Y, Chiashi S, Kohno M (2002) Chem Phys Lett 360:229
24. Méhn D, Fonseca A, Bister G, Nagy JB (2004) Chem Phys Lett 393:378